Supplement of The Cryosphere, 9, 1773–1795, 2015
http://www.the-cryosphere.net/9/1773/2015/
doi:10.5194/tc-9-1773-2015-supplement

The Cryosphere Open Access

Supplement of

Evolution of Ossoue Glacier (French Pyrenees) since the end of the Little Ice Age

R. Marti et al.

Correspondence to: R. Marti (renaud.marti@gmail.com)

Contents

1 Study site

Fig. 1) shows the Ossoue Glacier hypsometry.

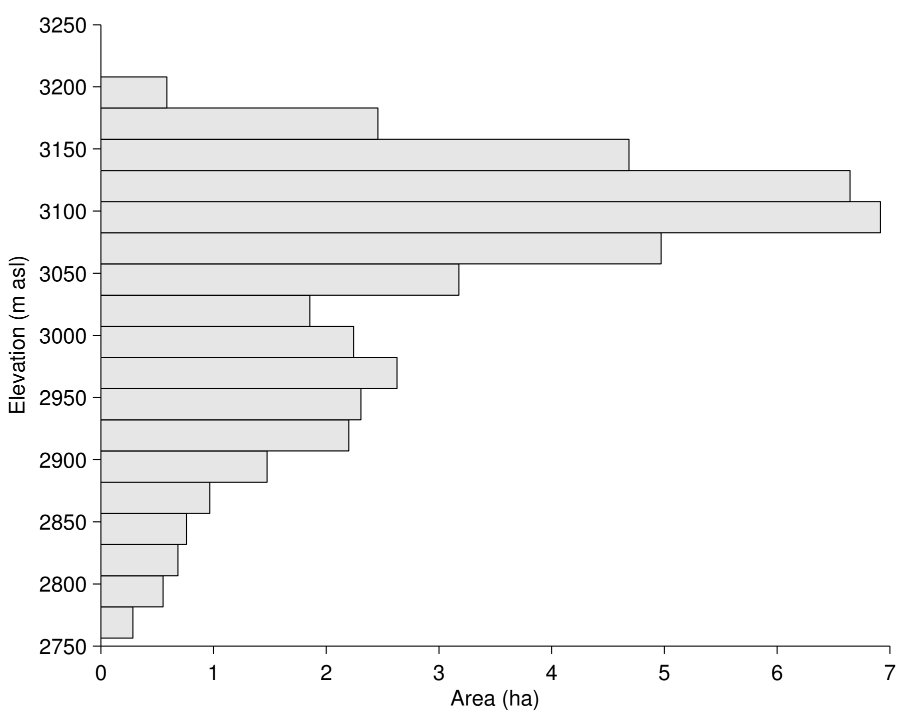

Figure 1: Ossoue Glacier hypsography in 25 m bins (2013).

The equilibrium line altitude (ELA) is a delicate concept in the case of Ossoue Glacier since there are only three occurrences of positive mass balance in the stake measurements dataset, if we except 2012–2013 (88 measurements over 2001-2012). We extrapolated an ELA value by computing the altitude of a zero mass balance using a least-squares linear fit of the stake mass balances as a function of elevation for each year (2002–2013). We found four years for which the regression coefficient R^2 is greater than 0.6 (Fig. 2). The median value of the ELA for these years is 3190 m a.s.l. (glacier maximal elevation is 3210 m a.s.l.).

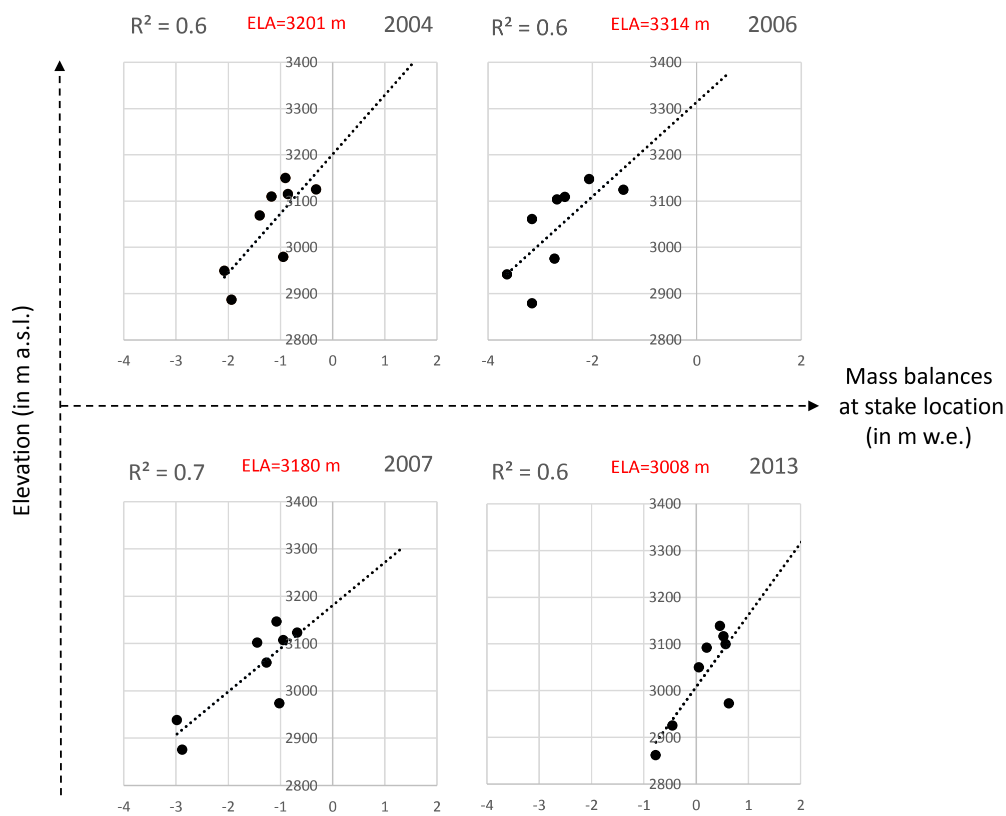

Figure 2: Linear fit of the Ossoue Glacier stakes mass balances as a function of elevation for year 2004, 2006, 2007, and 2013.

2 Errors measurements in mass balance calculation

2.1 DEM assessments

The map from 1924 was geo-referenced by extracting GCPs from a digital reference map at 1 : 25 000 scale (IGN Scan 25). For the 1948 and 1983 maps, the coordinates of the graticule intersections registered on the paper map allowed a direct geo-referencing of the scanned maps. The estimated accuracy in planimetry is 5 m for the 1924 map and 2 m for the 1948 and 1983 maps.

Topographic maps and georeferenced orthoimages (outlines) were assessed in planimetry using a 2010 aerial image orthorectified by the IGN as reference. We associated a random error to outline positions due to glacier margin interpretation, resolution or scale of the documents. From these errors, we generated buffers to estimate randoms errors in area, most likely resulting in error overestimations Hoffman et al. (2007). We estimated the randoms errors in cave height with respect to the glacier surface and in glacier front position based on a subjective assessment of the reliability of the observations as reported in the historical documents. We calculated total random errors in length, area and height (Villa-Russell) variations registered between two dates t_1 and t_2 by calculating the root sum of squares of each random errors:

$$\sigma_{\text{metric.total.PoR}} = \sqrt{\sigma^2_{\text{metric.}t_1} + \sigma^2_{\text{metric.}t_2}} \tag{1}$$

To scale the error to an annualized value of a N-years period of record (with $N = t_2 - t_1$), we considered two cases: (i) if the metric value at t_2 was deduced from the metric value at t_1, then we divided by $\sqrt{N}$ (e.g., in the case of the field measurements on the glacier front), or (ii) if both metric values were calculated independently, we divided by N (e.g., in areas variations based on diachronic aerial images).

2.2 Geodetic mass balance errors estimation

The differences between the DEM and the DGPS elevation values were normally distributed for 1948, 1983 and 2013. The mean elevation difference found for each DEM was noted as ϵ_{bias} ($\epsilon_{\text{bias.1948}} = -1.8$ m, $\epsilon_{\text{bias.1983}} = -1.4$ m, and $\epsilon_{\text{bias.2013.}P} = -1.37$ m for the 2013 Pléiades DEM) and was uniformly added to all the elevation values. For the 1924 DEM, the elevation differences did not follow a normal distribution and it was not possible to determine the elevation bias (noted as $\epsilon_{\text{bias.1924}}$). Hence, no correction was applied to this DEM. The SD of the elevation difference values on stable areas was considered as to be a representative value of the vertical random error and was noted as σ_{bias}. The random error term due to the interpolation process was calculated to be 0.5 m for 2011 and 2013 DGPS data.

We calculated an error term σ_{dc} associated with the uncertainty range due to density conversion. For every period, we considered an additional systematic error term ϵ_t due to the time lag between the raw data acquisition date and the first day of the next hydrological year, fixed to 1 October (when the elevation surface is expected to reach its annual minimum). The error ϵ_t was computed by multiplying the mean ablation rate observed during this period of the year over 2001–2013 (from stake measurements) by the duration of the time lag. At this stage we preferred to keep this term as an error rather than correcting the mass balance value, using a floating-date system (Cogley et al., 2011).

Following Zemp et al. (2013) the mean annual systematic error may be expressed as:

$$\overline{\epsilon_{\text{geod.total.a}}} = \frac{\epsilon_{\text{geod.total.PoR}}}{N} = \frac{\epsilon_{\text{geod.DEM.PoR}}}{N} \tag{2}$$

$$= \frac{\epsilon_{\text{bias}} + \epsilon_t}{N} \tag{3}$$

where PoR is period of record and N is the number of years in the PoR. After co-registration ϵ_{bias} is assumed to be 0, and therefore:

$$\overline{\epsilon_{\text{geod.total.a}}} = \frac{\epsilon_t}{N} \tag{4}$$

The mean annual random error may be expressed following (Zemp et al., 2013):

$$\overline{\sigma_{\text{geod.total.a}}} = \frac{\sigma_{\text{geod.total.PoR}}}{N} = \frac{\sqrt{\sigma^2_{\text{geod.DEM.PoR}}}}{N} \tag{5}$$

$$= \frac{\sqrt{\sigma^2_{\text{coreg}} + \sigma^2_{\text{dc}}}}{N} \tag{6}$$

Note that for scaling random errors at annual time steps, division is by the number of years (Zemp et al., 2013). The values of ϵ_{bias}, ϵ_t, σ_{coreg}, σ_{dc} and the resulting errors in DEM differences are given in Table 2. Annualized systematic and random errors are presented in Table in the paper.

2.3 Glaciological mass balances errors estimation

Annual systematic and random errors in the glaciological data series can be expressed as follows (Zemp et al., 2013):

$$\overline{\epsilon_{\text{glac.total.a}}} = \frac{\epsilon_{\text{glac.PoR}}}{N} \tag{7}$$

$$\overline{\sigma_{\text{glac.total.a}}} = \frac{\sum_{t=1}^{N} \sigma_{\text{glac.a.PoR}}}{\sqrt{N}} \tag{8}$$

$$= \frac{\sqrt{\sum_{t=1}^{N} \sigma^2_{\text{glac.point.}t} + \sigma^2_{\text{glac.spatial.}t} + \sigma^2_{\text{glac.ref.}t}}}{\sqrt{N}} \tag{9}$$

where PoR indicates the period of record, N is number of years in the PoR and point refers to the field measurement at the location point, spatial to spatial integration, and ref to the changing glacier area over time.
We estimated an annual systematic error of $\epsilon_{\text{gla.total.a}} = +0.14\,\text{m w.e.}$
By neglecting the error term $\sigma_{\text{glac.ref.a}}$ due the changes in glacier area, we estimated an annual total random error of $\sigma_{\text{glac.total.a}} = 0.85\,\text{m w.e.}$

2.3.1 Systematic error $\epsilon_{\text{glac.total.a}}$

The value of $\epsilon_{\text{glac.total.a}}$ was computed from the DPGS surveys performed in 2006 and 2011 as follows: (i) we calculated the mean elevation difference between both DEMs over polygons 1 to 4 (only these sectors were covered in 2006); and (ii) we calculated a mean geodetic mass balance assuming a density of $900\,kg\,m^{-3}$. We compared this geodetic mass balance to the corresponding glaciological mass balance. We obtained a difference of $-0.68\,\text{m w.e.}$ for $N = 5\,\text{years}$, which gives $\epsilon_{\text{gla.total.a}} = +0.14\,\text{m w.e.}$

2.3.2 Random error due to the field measurements $\sigma_{\text{glac.point.a}}$

We estimated random errors due to the field measurements following the guidelines provided by Gerbaux et al. (2005). Given that only three occurrences of positive mass balance were observed over the whole period of record (88 measurements), the entire glacier was considered as an ablation zone over this period for the estimation of the errors (i.e we neglected the errors associated with the residual snow from the previous year). The mean annual error in the specific mass balance is $\sigma_{\text{glac.point.a}} = 0.15\,\text{m w.e.}$ The specific mean winter mass balance error is $\sigma_{\text{glac.point.w}} = 0.35\,\text{m w.e.}$ (Tab. 4).

2.3.3 Random error due to the spatial integration $\sigma_{\text{glac.spatial.a}}$

Next, we estimated the random error due to the spatial integration $\sigma_{\text{glac.spatial.a}}$ to compute the glacier-wide glaciological mass balance from the specific mass balances. To do so we used the DEMs made from the DGPS surveys performed in 2011 and 2012, as if each pixel was a (virtual) stake. For every polygon 1 to 6 (only these polygons were surveyed), we calculated the variance of the differences between both DEMs. The six variances values were aggregated based on Eq. (4) of the manuscript, after rescaling the area weights. We obtained a mean value of $0.88\,\text{m w.e.}$ However, this error value is likely too high, because, in part, it propagates the errors included in the DGPS DEMs, and also introduce others terms in the error calculation: the internal and basal mass balances, and the ice mass variations due to the ice flow. Therefore, we took $\sigma_{\text{glac.spatial.a}} = 0.7\,\text{m w.e.}$

3 Ice depth measurements

3.1 Survey protocol

Three longitudinal profiles (W–E) running from the top to the slope transition of the glacier and four transverses profiles (N–S) were surveyed. The horizontal step was 0.5 m. The topography was acquired in real-time using a Leica DGNSS. In the radargrams strong reflectors identified at long two-way traveltimes were assumed to be the glacier bed. Hyperbolic features were used for electromagnetic (EM) velocity determination. An EM velocity of 0.16 m.ns $^{-1}$ was determined for the ice and was used to migrate the data. The thickness of the glacier was determined along the profiles at an horizontal resolution of 10 m. At the glacier margins the thickness was assumed to be zero (Saintenoy et al., 2013). The glacier thickness and surface elevation in 2006 were interpolated by ordinary kriging after second order trend removal (ESRI ArcGIS®, Geostatistical Analyst tool). Subsequently a map of the subglacial bedrock elevation was generated. Based on the standard error map associated with kriging, we excluded the area in the prediction map where the kriging error was greater than $\sigma_{\mathrm{krig}} = 10$ m.

3.2 Error estimations in ice depth measurements

The mean random error for the subglacial elevation was calculated as follows:

$$\sigma_{\mathrm{subglacial.total}} = \sqrt{\sigma^2_{\mathrm{GPR}} + \overline{\sigma_{\mathrm{krig}}}^2 + \sigma^2_{\mathrm{DEM.2006}}} \tag{10}$$

where σ_{GPR} is the spatial resolution of the survey (2 m), estimated from the spacing of the antenna elements, $\overline{\sigma_{\mathrm{krig}}}$ is the mean error from the kriging (6 m) and $\sigma_{\mathrm{DEM.2006}}$ the random error of the 2006 DEM (1.5 m). We obtained: $\sigma_{\mathrm{subglacial.total}} = 6.5$ m. The same mean error was used in the ice thickness determination in 2013 (i.e. we neglected the error introduced by the 2013 DEM). The kriging error associated with the maximum ice depth recorded in 2006 is $\sigma_{\mathrm{krig.max}} = 10$ m. Therefore, we propagated these errors into the 2013 maximum ice thickness (same location) and we calculated an error value of 10.3 m.

References

Cogley, J. G., Hock, R., Rasmussen, L. A., Arendt, A. A., Bauder, A., Jansson, P., Braithwaite, R. J., Kaser, G., Möller, M., Nicholson, L., Zemp, M.: Glossary of Glacier Mass Balance and Related Terms, Paris, UNESCO-IHP (IHP-VII Technical documents in hydrology, 86, IACS contribution 2), 2011.

Gerbaux, M., Genthon, C., Etchevers, P., Vincent, C., and Dedieu, J. P.: Surface mass balance of glaciers in the French Alps: distributed modeling and sensitivity to climate change, J. Glaciol., 51, 561–572, doi:10.3189/172756505781829133, 2005.

Hoffman, M. J., Fountain, A. G., and Achuff, J. M.: 20th-century variations in area of cirque glaciers and glacierets, Rocky Mountain National Park, Rocky Mountains, Colorado, USA, Ann. Glaciol., 46, 349–354, doi:10.3189/172756407782871233, 2007.

Saintenoy, A., Friedt, J.-M., Booth, A. D., Tolle, F., Bernard, E., Laffly, D., Marlin, C., and Griselin, M.: Deriving ice thickness, glacier volume and bedrock morphology of the Austre Lovenbreen (Svalbard) using Ground-penetrating Radar, arXiv preprint, arXiv:1306.2539, available at: `http://arxiv.org/abs/1306.2539` (last access: 8 April 2015), 2013.

Zemp, M., Thibert, E., Huss, M., Stumm, D., Rolstad Denby, C., Nuth, C., Nussbaumer, S. U., Moholdt, G., Mercer, A., Mayer, C., Joerg, P. C., Jansson, P., Hynek, B., Fischer, A., Escher-Vetter, H., Elvehøy, H., and Andreassen, L. M.: Reanalysing glacier mass balance measurement series, The Cryosphere, 7, 1227–1245, doi:10.5194/tc-7-1227-2013, 2013.

4 Supplementary tables: Ossoue Glacier reconstruction data and meta-data

4.1 Ossoue Glacier characteristics

Table 1: Characteristics of Ossoue Glacier.

	Name	Earlier names	Id Inventory
Identification	Ossoue Glacier	Aussoue	WGMS 2867
	Glacier d'Ossoue	Grand glacier de Montferrat	RGI 40-11.03864
		Vignemale	
Location	Geographic coordinates	Mountain range	Massif
	$42^o46'15''$	French Pyrenees	Vignemale
Glacier type	Primary class	Form	Frontal characteristics
	Mountain glacier	Cirque glacier	Double lobe, mainly clean ice
Dimension	Max. Length	Max. width	Area
	1400 m	400 m	0.45 km^2 (2011)
Hypsometry	Elevation range	Elevation mean	Elevation median
	2755–3210 m a.s.l.(2013)	3046 m a.s.l. (2013)	3076 m a.s.l. (2013)
Hydrography	Gave d'Ossoue	Gave de Pau	Adour River
Geomorphology	Nature of bedrock	Moraines	East-oriented cirque
	Limestone marble of Devonian	Visible lateral moraines	
		out of contact	

4.2 Meta-data of Ossoue Glacier volumetric measurements errors

Table 2: Meta-data of Ossoue Glacier volumetric measurements errors in m w.e. Mean elevation bias ϵ_z and SD σ_{coreg} are based on DGPS points surveyed on the deglaciated margin. The symbol * means that the bias was removed from the final DEM and was not taken into account in the total error. ϵ_t refers to the systematic error due to the timelag between the survey date and 1 October. The term σ_{dc} refers to the density conversion error. The last columns are the sums of systematic and random errors for the period of record (PoR). The propagation law is applied for random errors (root sum of squares).

Derived 2 m-DEM	DEM t_1	DEM t_2	Errors on DEMs Differences				
$t_1 - t_2$	(ϵ_z; σ_{coreg})	(ϵ_z; σ_{coreg})	ϵ_{t_1}	ϵ_{t_2}	σ_{dc}	$\epsilon_{total.PoR}$	$\sigma_{total.PoR}$
1924–1948	($\epsilon_{z.1924}$; 8.6)	(−1.8*; 2)	+1.71	+0.94	–	2.65 + $\epsilon_{bias.1924}$	8.8
1948–1983	(−1.8*; 2)	(−1.4*; 1.6)	+0.94	+1.41	0.3	2.35	2.6
1983–2013 Pléiades	(−1.4*; 1.6)	(−1.37*; 1.8)	+1.41	+0.42	1	1.83	2.6
1983–2013 DGPS	(−1.4*; 1.6)	(0; 0.6)	+1.41	0	1	1.41	1.9

4.3 Meta-data of Ossoue Glacier glaciological measurements

Table 3: Topographic characteristics (2013) by glaciological sectors (polygons) S_k, where k is the stake number.

	S_1	S_2	S_3	S_4	S_5	S_6	S_7	S_8
Mean elevation	3151 m	3115 m	3093 m	3100 m	3060 m	2981 m	2917 m	2862 m
Elevation range	95 m	65 m	63 m	77 m	105 m	94 m	81 m	192 m
Mean aspect	East	South-east	East	North-east	East	East	East	East
Mean slope	12.4^o	13.2^o	8^o	12.5^o	10.7^o	18.3^o	23.5^o	25.1^o
Area (Ha) in 2011	8.54	4.71	4.74	4.22	7.9	7.35	2.7	5.12
Weighting (since 2011)	0.18	0.11	0.11	0.11	0.16	0.16	0.06	0.11

4.4 Ossoue Glacier glaciological field error measurements

Table 4: Errors in field measurements at specific sites for winter and annual mass balance measurements, based on estimations by Gerbaux et al. (2005). In the case of Ossoue Glacier, we have considered the entire glacier as an ablation zone, which explains the null value associated with the determination of the transition between two consecutive years.

b_w measurements	Errors (in m w.e.)
Determination of surface level	0.1
Determination of transition between two consecutive years	0
Density measurements	0.05
Snow probing	0.2
Total in b_w measurements	0.35 m w.e.
$b_{glac.a}$ measurements	Errors (in m w.e.)
Stake emergence measure	0.04
Determination of surface level	0.1
Density measurement	0.01
Total in $b_{glac.a}$ measurements ($\sigma_{glac.point}$)	0.15 m w.e.

4.5 Ossoue Glacier metrics variations: length, area, and thickness at Villa Russel cave

Table 5: Ossoue Glacier length variations. The annualized variations marked with the index (*n.s.*) after the value are considered as not significant respect to the annualized error.

Year	Length (m)	Length variation (m)	Annualized variation ($m\,yr^{-1}$)	Annualized error $\sigma_{\mathrm{len.a}}$ ($m\,yr^{-1}$)	Percentage respect to 1850 length (%)
1850	2415.8	–	–	–	100.0
1874	2148.8	−267	−11.1	0.6	88.9
1885	2093.8	−55	−5	1.3	86.7
1889	2073.8	−20	−5	3.5	85.8
1890-91-92	2073.8	0	0 (n.s.)	14.1	85.8
1894-95-99	2062.8	-11	-11 (n.s.)	14.1	85.4
1904	1973.8	−89	−17.8	6.3	81.7
1905	1950.8	−23	−23.0	14.1	80.8
1906-07-08-09-10-11	1950.8	0	0 (n.s.)	14.1	80.8
1921	1982.3	31.5	3.2 (n.s.)	4.5	82.1
1927	2007.8	25.5	4.3 (n.s.)	5.8	83.1
1928	1961.6	−46.2	−46.2	14.1	81.2
1935	1916.8	−44.8	−6.4	4.2	79.3
1945	1906.8	−10	−1 (n.s.)	2.2	78.9
1946	1905.3	−1.5	−1.5 (n.s.)	7.1	78.9
1950	1841.8	−63.5	−15.9	3.5	76.2
1953	1823.8	−18	−6	4.1	75.5
1957	1680.8	−143	−35.8	2.8	69.6
1962	1591.8	−89	−17.8	2.2	65.9
1970	1617.8	26	3.3	1.3	67.0
1982	1742.8	125	10.4	0.3	72.1
1983	1747.8	5.0	5	4.2	72.3
1985-86	1747.8	0	0 (n.s.)	2.1	72.3
1990	1681.1	−66.7	−16.7	1.1	69.6
1995	1588.1	−93	−18.6	0.8	65.7
2001	1537.5	−50.6	−8.4	0.5	63.6
2002	1531.8	−5.7	−5.7	1.4	63.4
2003	1527.8	−4	−4	1.4	63.2
2004	1523.5	−4.3	−4.3	1.4	63.1
2005	1496	−27.5	−27.5	1.4	61.9
2006	1483	−13	−13	1.4	61.4
2007	1417.5	−65.5	−65.5	1.4	58.7
2008	1417	−0.5	−0.5 (n.s.)	1.4	58.7
2009	1411.5	−5.5	−5.5	1.4	58.4
2010	1411.5	0	0 (n.s.)	1.4	58.4
2011	1412	0.5	0.5 (n.s.)	1.4	58.4
2012	1400	−12.0	−12	1.4	58.0
2013	1400	0	0 (n.s.)	1.4	58.0

Table 6: Ossoue Glacier areal changes. Variations and annualized errors are calculated between two consecutive dates. The annualized variations marked with the index (*n.s.*) after the value are considered as not significant respect to the annualized error.

Year	Area (ha)	Area variation (ha)	Annualized variation ($ha\,yr^{-1}$)	Annualized error $\sigma_{\text{area.a}}$ ($ha\,yr^{-1}$)	Percentage respect to 1850 area (%)
1850	112.5	–	–	–	100 %
1924	89.8	−22.7	−0.31	0.15	79.8 %
1948	80.4	−9.4	−0.39	0.24	71.5 %
1950	73	−7. 4	−3.7	3.2	64.9 %
1953	72.8	−0.2	−0.07 (n.s.)	2.36	64.7 %
1983	76.9	4.1	0.14 (n.s.)	0.21	68.4 %
1988	70	−6.9	−1.38	1.13	62.2 %
1992	62	−8	−2	1.41	55.1 %
2002	58	−4	−0.4 (n.s.)	0.45	51.6 %
2004	55	−3	−1.5	1.41	48.9 %
2006	50	−5	−2.5	1.41	44.4 %
2007	46	−4	−4	2.82	40.9 %
2011	45	−1	−0.25 (n.s.)	0.71	40 %
2013	45	0	0	–	40 %

Table 7: Height variations (m) at Ossoue Glacier between the Villa Russell cave threshold and the glacier surface. The annualized variations marked with the index (*n.s.*) after the value are considered as not significant respect to the annualized error.

Year	Heigth (m)	Height variation (m)	Annualized variation ($m\,yr^{-1}$)	Annualized error $\sigma_{\mathrm{VR.a}}$ ($m\,yr^{-1}$)
1881-82	0	0	0 (n.s.)	1.1
1883	−3.5	−3.5	−3.5	1.1
1884	0	3.5	3.5	1.1
1885	1	1	1.0 (n.s.)	1.1
1886	4	3	3.0	1.1
1887	6	2	2.0	1.1
1888	0	−6	−6.0	1.1
1889	6	6	6.0	1.1
1890-91-92-93-94	6	0	0 (n.s.)	1.1
1895	0	−6	−6.0	1.1
1898	−11	−11	−3.7	0.4
1901	−1.5	9.5	3.2	0.3
1902	−3.5	−2	−2.0	0.7
1904-05	−4.5	−1	−0.5	0.4
1906	−3.75	0.25	0.3 (n.s.)	0.7
1907-08	4	7.75	7.8	0.7
1909-10	6	2	2.0	0.7
1911	4	−2	−2.0	0.7
1913	5.5	1.5	0.8	0.4
1927	0.2	−5.3	−0.4	0.1
1937	−3	−3.2	−0.3	0.1
1945	−12	−9	−1.1	0.1
1950	−13.5	−1.5	−0.3	0.1
1952	−2	11.5	5.8	0.4
1953	0	2	2.0	0.7
1967	2	2	0.1	0.1
1983	−0.3	−2.3	−0.1	0.1
1985	−3.6	−3.3	−1.7	0.4
1986	−5	−1.4	−1.4	0.7
1987	−8	−3	−3.0	0.7
1991	−1	7	1.8	0.2
2002	−7	−6	−0.5	0.1
2003	−7.9	−0.9	−0.9	0.7
2004-05	−7.5	0.4	0.4 (n.s.)	0.7
2006	−7.3	0.3	0.3 (n.s.)	0.7
2007	−11.3	−4	−4.0	0.7
2008	−6.9	4.4	4.4	0.7
2009	−7.5	−0.6	−0.6 (n.s.)	0.7
2010	−10.2	−2.7	−2.7	0.7
2011	−14	−3.8	−3.8	0.7
2012	−16.5	−2.5	−2.5	0.7
2013	−12.2	4.3	4.3	0.7